Afghanistan Journal of Infectious Diseases
AJID
https://ajid.ghalib.edu.af/index.php/ajid

January 2026, Vol. 4, No.1, pp:114-126

COVID-19 Transmission Dynamics in Afghanistan: Insights from Compartmental Models on Vaccination and Control

*Amanullah Nabavi, Aminullah Hussaini

Department of Mathematics, Natural Science Faculty, Bamayan University, Bamyan City, Afghanistan

ARTICLE INFO

Type: Original Article
Received: 24/08/2025
Accepted: 30/12/2025

*Corresponding Author:
E-mail address:
nabave786@gmail.com

To cite this article:
Nabavi A, Hussaini A. COVID-19 Transmission Dynamics in Afghanistan: Insights from Compartmental Models on Vaccination and Control. Afghan J Infect Dis. 2026; 4(1): pp: 114-126.

DOI:
https://doi.org/10.60141/ajid.135

ABSTRACT

Background: The COVID-19 pandemic has created substantial public health challenges worldwide, with Afghanistan facing unique vulnerabilities due to limited healthcare infrastructure and uneven vaccine coverage. Understanding the transmission dynamics of COVID-19 in this context is essential for designing effective intervention strategies.
Methods: Epidemiological data, including confirmed cases, mortality, and vaccination rates, were obtained from Our World in Data. Vaccination data were available from February 22, 2021, to December 31, 2023, and mortality rate estimation was based on data spanning April 1, 2020, to June 29, 2025. We developed a deterministic SEVIR compartmental model capturing susceptible, exposed, vaccinated, infectious, and recovered populations. The model was analyzed for biological feasibility, and key parameters, including the vaccination and mortality rates, were estimated from the data. Sensitivity analyses were conducted to determine the influence of parameters on disease progression. The basic reproduction number ($\mathcal{R}_0$) was derived analytically, and stability analysis of the disease-free equilibrium was performed.
Results: Model simulations indicate that the current vaccination rate in Afghanistan is insufficient to eliminate COVID-19. Doubling vaccination coverage could significantly reduce infection prevalence, while achieving herd immunity would require vaccinating approximately 86% of the population. Sensitivity analyses highlighted the critical role of vaccination and transmission rates in controlling disease spread. The disease-free equilibrium is locally stable whenever $\mathcal{R}_0 < 1$, confirming the theoretical feasibility of disease elimination.
Conclusion: These findings provide comprehensive insights into COVID-19 dynamics in Afghanistan and offer evidence-based guidance for public health policymakers to optimize vaccination strategies and mitigate the ongoing impact of the pandemic.

Keywords: Afghanistan, COVID-19, Compartmental modeling, Vaccination rate

Introduction

Coronavirus disease 2019 (COVID-19), caused by the SARS-CoV-2 virus, remains a major global health challenge, primarily transmitted through respiratory droplets and contact with contaminated surfaces. Its clinical presentation ranges from mild symptoms, such as fever, cough, and fatigue, to severe respiratory distress and life-threatening complications (1–3).

First identified in Wuhan, China, in late 2019, COVID-19 spread rapidly worldwide, prompting unprecedented public health interventions and profoundly affecting daily life. The WHO declared COVID-19 a pandemic, with over 507.5 million confirmed cases and 6.22 million deaths reported globally across more than 200 countries and territories as of April 25, 2022 (4). In Afghanistan, the first case was confirmed on February 24, 2020 (5). Since then, approximately 235,000 infections and over 8,000 deaths have been reported (6). The pandemic's impact has been amplified by a fragile healthcare system and delayed vaccination efforts, making COVID-19 one of the leading causes of mortality in 2021 (7).

While vaccination is a key strategy to control COVID-19, practical challenges limit its effectiveness. Mass immunization is constrained by vaccine supply, distribution logistics, medical contraindications, and public hesitancy. For example, a substantial fraction of the Afghan population is reluctant to receive COVID-19 vaccines (8). Moreover, partially effective vaccination programs targeting only subsets of at-risk populations can, under certain conditions, exacerbate outbreak severity (9).

Some studies have analyzed COVID-19 dynamics in Afghanistan. Movaheedi et al. used a DINNs–SEIRV framework to reconstruct epidemic waves and estimated time-varying transmission parameters (10). Awan et al. applied Exponential Smoothing to forecast case trends, showing continued growth (11). Husseini and Kamil estimated fatality, recovery, and transmission rates while noting data-related underestimation (5). Besides, Dar et al. examined the mortality patterns using probabilistic methods across Afghanistan and Pakistan (12). While these works provide valuable insights, they leave key policy questions unanswered—particularly whether a controllability threshold exists and, if such targets cannot be fully met, which intervention yields the greatest reduction in transmission under real-world constraints. In Afghanistan, limited adherence to masking and distancing and substantial economic and logistical barriers to mass vaccination make full implementation of standard control measures impractical. Therefore, identifying which control strategy provides the highest impact when resources and compliance are restricted becomes essential.

We addressed this gap by evaluating the relative influence of major control measures within a deterministic model to guide policymakers toward the most effective, feasible interventions. In this study, the primary objective was to characterize the transmission dynamics of COVID-19 in Afghanistan through the development and analysis of a deterministic compartmental model using differential equation techniques, calibrated with vaccination and mortality data from Our World in Data. The model incorporates key contextual constraints—including limited healthcare capacity, economic challenges, and population-level behavioral factors—to evaluate the epidemiological impact of feasible intervention strategies, with particular emphasis on vaccination. By combining real-world data with a context-specific mathematical framework, the study provides policymakers with rigorous, evidence-based guidance for optimizing vaccination coverage and strategically timing public health interventions under operationally realistic conditions.

Materials and Methods

Model formulation

The total population, denoted by n, is partitioned into five mutually exclusive fractional subpopulations: susceptible (s), vaccinated (v), exposed (e), infectious (i), and recovered (r). Each individual belongs to exactly one compartment at any given time.

Susceptible individuals are those at risk of contracting the infection. Vaccinated individuals have received at least one dose of a COVID-19 vaccine, but immunity is not assumed to be absolute; they may still become infected at a reduced rate of $(1-\epsilon)$, where ϵ represents vaccine efficacy against infection. The exposed class consists of individuals infected but not yet infectious. Infectious individuals are capable of transmitting the disease to susceptible people. Recovered individuals have acquired immunity through vaccination, prior infection, or natural resistance.

Disease transmission is modeled through a bilinear mass-action term, βsi, indicating that the rate of new infections is proportional to the product of susceptible and infectious individuals. The model excludes environmental and vector-borne transmission, assuming that spread occurs exclusively via direct human-to-human contact. A homogeneous mixing assumption is applied, whereby all individuals have an equal probability of contacting one another. All parameters are considered constant in time. Reinfection is assumed to occur in constant rate. The compartmental structure of the model is illustrated in Figure 1.

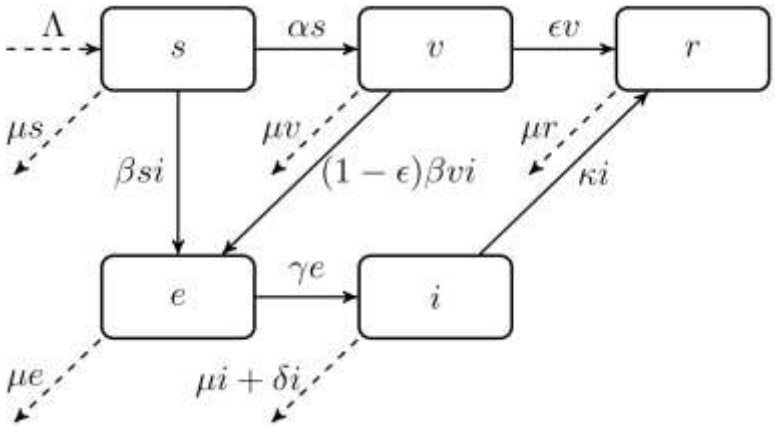

Figure 1: The flow diagram between compartments

Guided by this schematic and the assumptions outlined above, the system of governing equations is formulated as follows:

$$\begin{aligned} \dot{s} &= \Lambda - \beta si - \alpha s - \mu s, \\ \dot{e} &= \beta si + (1-\epsilon)\beta vi - \gamma e - \mu e, \\ \dot{v} &= \alpha s - (1-\epsilon)\beta vi - \epsilon v - \mu v, \\ \dot{i} &= \gamma e - \kappa i - \delta i - \mu i, \\ \dot{r} &= \epsilon v + \kappa i - \mu r. \end{aligned} \quad (Eq1)$$

Parameter Definitions

The parameters used in the model (Eq1) are summarized in Table 1.

Table 1: The summary of parameters

Symbol	*Description*	*Source*	*Value*
Λ	Recruitment rate of susceptible individuals into the population	Assumed	0.00971
β	The rate at which infectious individuals transmit the disease to susceptible individuals	(24-26)	[0.3, 0.5]
α	Rate at which susceptible individuals are vaccinated and move into the vaccinated class	Estimated	0.00325
μ	Natural death rate, assumed equal across all compartments	(14)	0.000016
ϵ	Vaccine efficacy (ϵ) represents the reduction in susceptibility to infection among vaccinated individuals. It is assumed to be below average, reflecting the greater affordability and availability of lower-priced, lower-efficacy vaccines in Afghanistan.	(15-17)	0.75
γ	The inverse of the mean latent period, determining the rate of progression from exposed to infectious	(21)	0.33
δ	COVID-19-induced death rate of infectious individuals	estimated	0.0025
κ	Recovery rate of infectious individuals	(22)	0.196

The parameter Λ represents the recruitment rate, defined as the total inflow into the susceptible class arising from natural births, immigration into the country, the return of individuals who lose infection-induced immunity, and the inflow generated by vaccine inefficacy (i.e., vaccinated individuals who do not acquire sufficient protection). For simplicity and model fitting, we assume $\Lambda = 0.00971$. The contribution from births is estimated using Afghanistan's crude birth rate in 2023, reported as 35.437 births per 1,000 population per year (13). This corresponds to

$$\frac{35.437}{1000 \times 365} \approx 9.71 \times 10^{-5} = 0.0000971,$$

the remaining portion of Λ accounting for the inflow generated by loss of immunity after recovery, immigration into the country, and vaccine inefficacy (i.e., vaccinated individuals who fail to acquire adequate protection). The parameter μ corresponds to the natural death rate. In short-term epidemic modeling, μ is typically negligible because of its small magnitude relative to epidemic-related rates. The natural daily death rate (μ) was estimated using national mortality statistics. According to Macrotrends (14), the crude death rate in Afghanistan is approximately 5.8 deaths per 1,000 population per year. Converting this to a daily rate yields $\mu = 5.8/(1000 \times 365) \approx 0.000016$ per person per day.

Vaccine efficacy against infection is denoted by ϵ. For COVID-19 vaccines, reported efficacy ranges from 70% to 95%, depending on vaccine type and circulating variants. For instance, Pfizer–BioNTech (BNT162b2, mRNA) demonstrated 95% efficacy (15), Moderna (mRNA-1273, mRNA) showed similar results (16), while Johnson & Johnson/Janssen (Ad26.COV2.S, adenovirus vector) demonstrated about 67% efficacy (17). Considering the reported vaccine efficacy levels and Afghanistan's limited economic capacity, access to high-efficacy vaccines is less likely due to their higher cost, while lower-efficacy vaccines are more accessible and affordable. Therefore, the vaccine efficacy was set to $\epsilon = 0.75$ to reflect this realistic scenario.

The incubation period is denoted by γ and varies across variants. The median incubation period was approximately 5.1 days for the ancestral Wuhan strain (18), 4 days for the Delta variant

(19), and 3 days for Omicron BA.1 (20). Following (21), we adopt an average incubation period of 3 days, corresponding to $\gamma \approx 1/3 \approx 0.33$.

The average infectious period also differs across variants. Based on (22), we assume a 7-day infectious period, which implies a recovery rate of $\kappa \approx 0.14$ per day.

The disease-induced death rate, δ, is determined from the case fatality rate (CFR) and the average infectious period. For instance, if the CFR is 1% and the infectious period is approximately 7 days, then $\delta \approx 0.0014$ per day. In more severe outbreaks, higher values of δ may occur (23). In this study, however, δ was estimated directly from reported data (see subsection mortality rate).

Analytical methods

Non-negativity Preservation and Boundedness

In the mathematical modeling of biological phenomena, positivity and boundedness are fundamental properties. Without these, the model may yield results that are biologically meaningless or impractical for real-world interpretation.

Let the initial conditions of system (Eq1) satisfy

$$s(0) \geq 0, \quad e(0) \geq 0, \quad v(0) \geq 0, \quad i(0) \geq 0, \quad r(0) \geq 0, \qquad \textit{(Eq2)}$$

and define the total population as

$$n(t) = s(t) + e(t) + v(t) + i(t) + r(t) + d(t).$$

Under these assumptions, the following properties hold for the solutions of system (Eq1).

Theorem 1 (Positive invariance of the feasible region). *For the system* (Eq1), *the feasible region* Ω *is defined as* $\Omega = \left\{(s, e, v, i, r) \in \mathbb{R}_+^5 : 0 \leq n \leq \frac{\Lambda}{\mu}\right\}$. Then, the region Ω is positively invariant under the flow induced by the system (Eq1); that is, any solution with initial condition in Ω remains in Ω for all $t \geq 0$.

Proof. From (Eq1), one can easily see that

$$\dot{n} = \Lambda - \mu n - \delta i.$$

In the absence of disease-induced mortality ($\delta = 0$), the above equation simplifies to

$$\dot{n} + \mu n = \Lambda,$$

which is a linear ordinary differential equation and under the initial condition $n(0) = n_0$ can be easily solved as

$$n(t) = \frac{\Lambda}{\mu} + n_0 e^{-\mu t}.$$

We see that $n(t) \to \frac{\Lambda}{\mu}$ as $t \to \infty$. Thus, for any $t \geq 0$ we have $0 \leq n(t) \leq \frac{\Lambda}{\mu}$. Therefore, the system (Eq1), is biologically meaningful.

Theorem 2. The solutions of system (Eq1) with the initial condition (Eq2) is non-negative for any $t \geq 0$. Additionally, the solutions are uniformly ultimately bounded

Proof

To prove the positivity of the solutions of the system we use contradiction approach. Let the positivity fails, then at least one variable becomes nonpositive at some time $t^* > 0$. For the first equation of the system, assume $s(t^*) = 0$ and $\dot{s}(t^*) < 0$. Then:

$$\dot{s} = \Lambda - \beta s i - (\alpha + \mu) s$$

at time t^* becomes as $\dot{s}(t^*) = \Lambda$, which is obviously greater than 0. Thus the assumption must not be true and therefore we must have $s(t) \geq 0$ for any $t \geq 0$.

Now, we turn our attention to the second equation. For some time $\tilde{t} > 0$, let $e(\tilde{t}) = 0$ and $\dot{e}(\tilde{t}) < 0$. Then, at time $\tilde{t}$, we get

$$\dot{e} = [\beta s + (1 - \epsilon)\beta v] i > 0,$$

when $s(\tilde{t}) > 0$, $v(\tilde{t}) > 0$, and $i(\tilde{t}) > 0$. This contradicts the assumption, thus $e(t) \geq 0$ must holds for any $t \geq 0$.

The positivity of all other variables can be obtained similarly. Therefore, all solutions of system (Eq1) are non-negative for all $t \geq 0$.

We know that $n \leq \frac{\Lambda}{\mu}$, and $n = s + e + v + i + r$, thus each solutions are bounded. This completes the proof.

Disease-Free Equilibrium (DFE)

In compartmental epidemiological modeling, the disease-free equilibrium (DFE) represents the state in which the infection is entirely absent from the population. Formally, this condition is expressed as

$$e(t) = 0, \quad i(t) = 0.$$

At this equilibrium, the population may consist of susceptible, vaccinated, or recovered individuals, but no one remains exposed or infectious. Substituting these conditions into system (Eq1) gives the equilibrium values

$$s = \frac{\Lambda}{\alpha+\mu}, \quad v = \frac{\alpha\Lambda}{(\alpha+\mu)(\epsilon+\mu)}, \quad r = \frac{\epsilon\alpha\Lambda}{\mu(\alpha+\mu)(\epsilon+\mu)}.$$

Thus, the DFE point is defined as

$$(\tilde{s}, \tilde{e}, \tilde{v}, \tilde{\imath}, \tilde{r}) = \left(\frac{\Lambda}{\alpha+\mu}, 0, \frac{\alpha\Lambda}{(\alpha+\mu)(\epsilon+\mu)}, 0, \frac{\epsilon\alpha\Lambda}{\mu(\alpha+\mu)(\epsilon+\mu)}\right)$$

The basic reproduction number

To derive meaningful public health insights from system (Eq1), it is necessary to compute the basic reproduction number, denoted by $\mathcal{R}_0$. This threshold parameter measures the average number of secondary cases generated by a single infectious individual in a fully susceptible population. Its calculation commonly relies on the Next Generation Matrix (NGM) method (27), where $\mathcal{R}_0$ is given by the spectral radius (dominant eigenvalue) of the product

$$FV^{-1},$$

where the matrices $\mathcal{F}$ and $\mathcal{V}$ represent the rates of new infections and transitions between compartments, respectively, and is obtained as

$$\mathcal{F} = \begin{pmatrix} \beta si + (1-\epsilon)\beta vi \\ 0 \end{pmatrix}, \quad \mathcal{V} = \begin{pmatrix} (\gamma+\mu)e \\ (\kappa+\delta+\mu)i - \gamma e \end{pmatrix}.$$

Thus, F and V are defined as their Jacobian matrices and is obtained as:

$$F = \begin{pmatrix} 0 & \beta s + (1-\epsilon)\beta v \\ 0 & 0 \end{pmatrix}, \quad V = \begin{pmatrix} \gamma+\mu & 0 \\ -\gamma & \kappa+\delta+\mu \end{pmatrix}.$$

After applying standard linear algebra techniques, the matrix is obtained as:

$$FV^{-1} = \begin{pmatrix} \frac{\beta\gamma[s+(1-\epsilon)v]}{(\gamma+\mu)(\kappa+\delta+\mu)} & \frac{\beta s+(1-\epsilon)\beta v}{\kappa+\delta+\mu} \\ 0 & 0 \end{pmatrix}.$$

Thus, the BRN is expressed as:

$$\mathcal{R}_0 = \frac{\beta\gamma\Lambda}{(\alpha+\mu)(\gamma+\mu)(\kappa+\delta+\mu)} + \frac{(1-\epsilon)\beta\alpha\gamma\Lambda}{(\alpha+\mu)(\epsilon+\mu)(\gamma+\mu)(\kappa+\delta+\mu)}. \quad \textit{(Eq3)}$$

The calculated basic reproduction number $\mathcal{R}_0$ quantifies the average number of secondary cases generated by a single infected individual in a completely susceptible population. The first term represents transmission among unvaccinated individuals, while the second accounts for breakthrough infections among vaccinated individuals with partial immunity. A value of $\mathcal{R}_0 > 1$ implies that the infection can persist and spread in the population, whereas $\mathcal{R}_0 < 1$ indicates that the disease will eventually die out.

Theorem 3. ***The DFE is locally asymptotically stable if*** $\mathcal{R}_0 < 1$.

Proof

The idea is to linearize the system (Eq1) around the DFE point using Jacobin matrix. Let $F_i, i = 1, \ldots, 6$ denote the right side and M be the Jacobin of the system. Therefore

$$M = \begin{pmatrix} -\beta i-\alpha-\mu & 0 & 0 & -\beta s & 0 \\ \beta i & -(\gamma+\mu) & (1-\epsilon)\beta i & \beta s+(1-\epsilon)\beta v & 0 \\ \alpha & 0 & -(1-\epsilon)\beta i-(\epsilon+\mu) & -(1-\epsilon)\beta v & 0 \\ 0 & \gamma & 0 & -(\kappa+\delta+\mu) & 0 \\ 0 & 0 & \epsilon & \kappa & -\mu \end{pmatrix}.$$

Now, the matrix M at the DFE point is denoted as M_{DFE} and is defined as

$$M_{DFE} = \begin{pmatrix} -\alpha-\mu & 0 & 0 & -\frac{\beta\Lambda}{\alpha+\mu} & 0 \\ 0 & -(\gamma+\mu) & 0 & \frac{\beta\Lambda}{\alpha+\mu}+\frac{(1-\epsilon)\beta\alpha\Lambda}{(\alpha+\mu)(\epsilon+\mu)} & 0 \\ \alpha & 0 & -(\epsilon+\mu) & -\frac{(1-\epsilon)\beta\alpha\Lambda}{(\alpha+\mu)(\epsilon+\mu)} & 0 \\ 0 & \gamma & 0 & -(\kappa+\delta+\mu) & 0 \\ 0 & 0 & \epsilon & \kappa & -\mu \end{pmatrix}.$$

The eigenvalues of matrix M_{DFE} are $-(\alpha+\mu)$, $-(\epsilon+\mu)$, $-\mu$, and the eigenvalues of the 2×2 matrix

$$\begin{pmatrix} -(\gamma+\mu) & \gamma \\ \frac{\beta\Lambda}{\alpha+\mu}+\frac{(1-\epsilon)\beta\alpha\Lambda}{(\alpha+\mu)(\epsilon+\mu)} & -(\kappa+\delta+\mu) \end{pmatrix}.$$

Since three of eigenvalues are negative, therefore, in order the eigenvalues of the matrix have negative real parts, the above 2×2 matrix must have negative trace and positive determinant (28). The negativity of the trace is obvious. For the determinant to be positive we get

$$(\gamma+\mu)(\kappa+\delta+\mu) > \frac{\beta\gamma\Lambda}{\alpha+\mu}+\frac{(1-\epsilon)\beta\alpha\gamma\Lambda}{(\alpha+\mu)(\epsilon+\mu)}.$$

Then, we get

$$1 > \frac{\beta\gamma\Lambda}{(\alpha+\mu)(\gamma+\mu)(\kappa+\delta+\mu)} + \frac{(1-\epsilon)\beta\alpha\gamma\Lambda}{(\alpha+\mu)(\epsilon+\mu)(\gamma+\mu)(\kappa+\delta+\mu)} = \mathcal{R}_0.$$

Thus, the DFE is locally asymptotically stable if $\mathcal{R}_0$ is strictly less than one. □

Results

Estimation of the Daily Vaccination Rate

Let C_t denote the cumulative number of vaccinated individuals up to day t, and let N represent the total population. The daily new vaccinations are computed as

$$\Delta C_t = C_t - C_{t-1}, \quad t = 2, \ldots, T, \quad \Delta C_1 = C_1.$$

If cumulative data are missing for some days, we apply *linear interpolation* to estimate the missing values, avoiding artificial spikes due to batch reporting.

The per-capita daily vaccination rate is then calculated as

$$\alpha_t = \frac{\Delta C_t}{N}.$$

To reduce the impact of reporting noise and irregularities, we smooth α_t using a 7-day moving average:

$$\tilde{\alpha}_t = \frac{1}{7}\sum_{i=t-3}^{t+3} \alpha_i.$$

Finally, a single average vaccination rate over the observation period is obtained as

$$\alpha = \frac{1}{T}\sum_{t=1}^{T} \tilde{\alpha}_t,$$

which can be used as a constant vaccination rate in compartmental models. Based on the data reported in (29), the average daily vaccination rate was estimated to be 0.00325 (Figure 2).

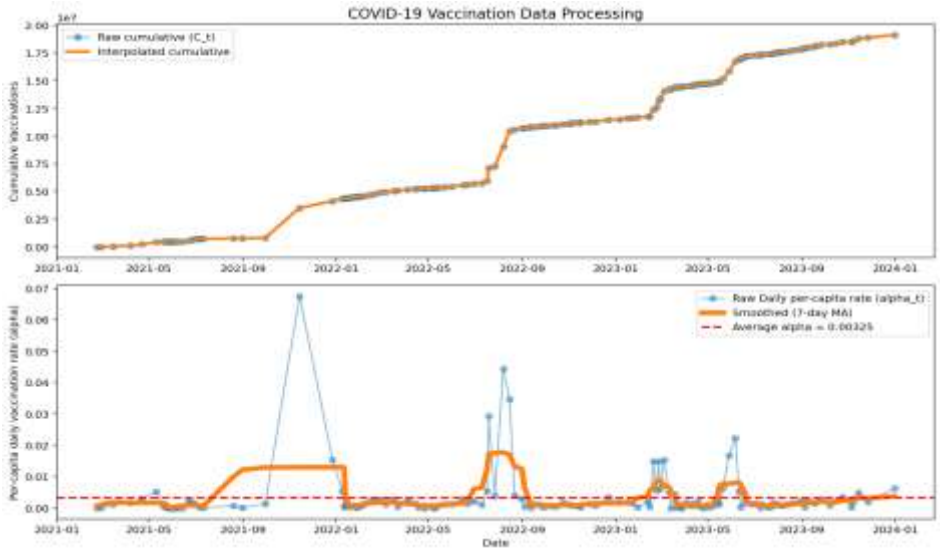

Figure 2: Graph of reported daily cumulative vaccinations, interpolated data, daily per-capita vaccination rate, 7-day smoothed average, and overall average

Mortality rate per day

We estimated the daily mortality rate using reported confirmed cases (C_t) and deaths (D_t) at day t ($t = 1, \dots, T$). The number of active infections was defined as

$$I_t = \sum_{s=t-L+1}^{t} C_s - \sum_{s=t-L+1}^{t} D_s,$$

with $L = 14$ days (30), reflecting the average infectious period. The day-specific mortality rate was then given by

$$\delta_t = \frac{D_t}{I_t},$$

while the overall period-average mortality rate was

$$\delta = \frac{\sum_{t=1}^{T} D_t}{\sum_{t=1}^{T} I_t}.$$

To reduce reporting noise and weekly fluctuations, we replaced C_t and D_t with their 7-day centered rolling averages,

$$\tilde{C}_t = \frac{1}{7}\sum_{k=-3}^{3} C_{t+k}\,, \qquad \tilde{D}_t = \frac{1}{7}\sum_{k=-3}^{3} D_{t+k},$$

and further smoothed the sequence δ_t itself using the same procedure, yielding a clean trajectory of mortality dynamics. Accordingly, the mortality rate was estimated as $\delta = 0.0025$ (Figure 3).

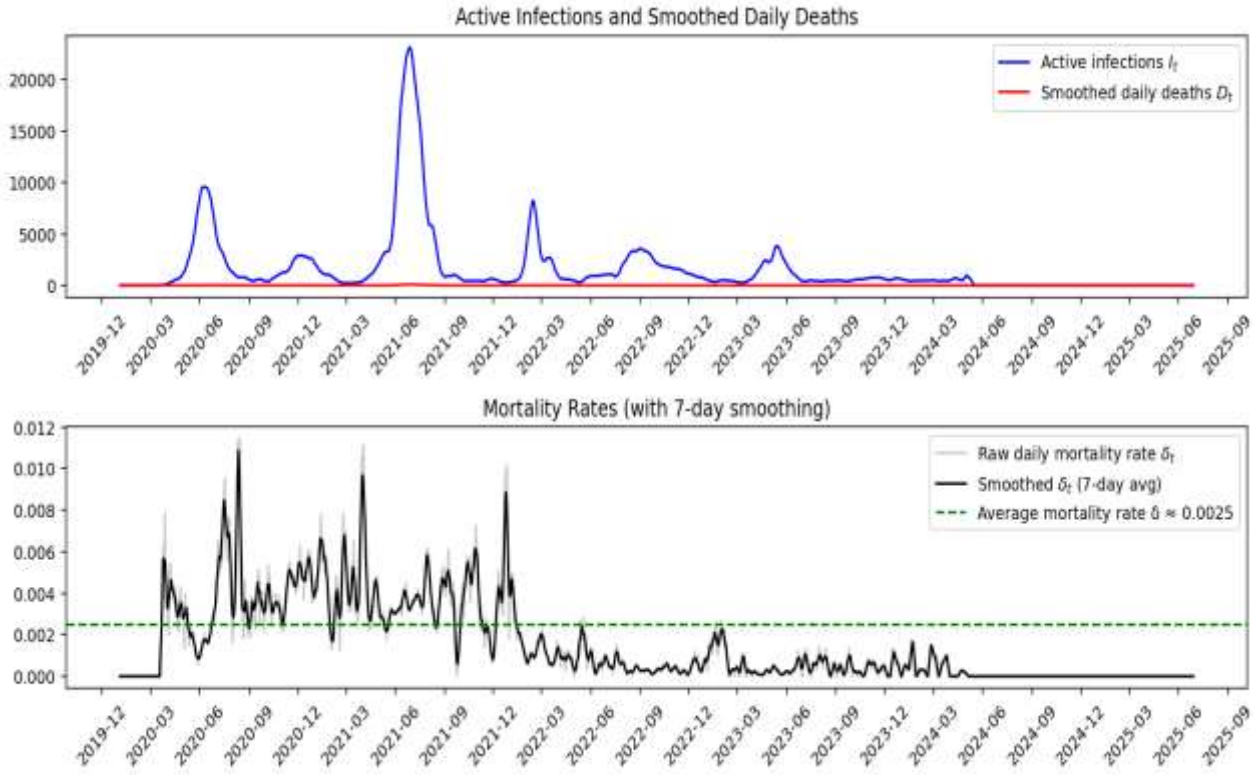

Figure 3: The daily reported rate

Sensitivity analysis

In order to understand the impact of each parameter on the dynamics of the system (Eq1), we need to perform a sensitivity analysis. The analysis tells us how much changes in parameter can considerably impact the outcome. Thus, we can decide to focus on which in order to control the disease. For this purpose, we use the normalized formula

$$S_p = \frac{p}{\mathcal{R}_0}\frac{\partial \mathcal{R}_0}{\partial p}.$$

The idea is such that we let one parameter to change and keep all others constant. After running a sensitivity analysis on (Eq3), we come to the conclusion that parameters β, Λ, α, and κ have the highest impact, respectively. On the other hand, however, we noticed that parameters δ, μ, ϵ, and γ have lowest impact on the system, respectively (Figure 4). We must note that a positive sensitivity index means that by increasing (decreasing) that parameter the amount of $\mathcal{R}_0$ increases (decreases), while negative sign means that increasing (decreasing) that parameter the amount of $\mathcal{R}_0$ decreases (increases). According to the sensitivity indices presented in Table 2, the parameters β and Λ each have a sensitivity index of 1, indicating that x % change in either parameter results in a corresponding x % change in $\mathcal{R}_0$. Conversely, the parameter α has a sensitivity index of -0.994, meaning that an x % increase (or decrease) in α leads to an approximate $0.994x$ % decrease (or increase) in the value of $\mathcal{R}_0$.

The sensitivity index of each parameter is depicted in figure 4. The baseline values are presented in Table 2.

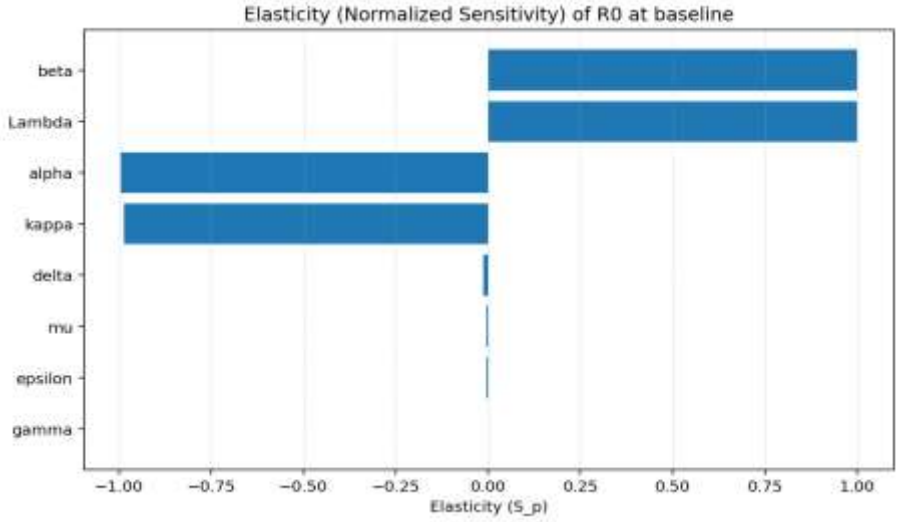

Figure 4: The sensitivity analysis bar of $\mathcal{R}_0$

Table 2: The baseline and sensitivity index of parameters

Parameter	$\boldsymbol{\beta}$	$\boldsymbol{\gamma}$	$\boldsymbol{\Lambda}$	$\boldsymbol{\alpha}$	$\boldsymbol{\mu}$	$\boldsymbol{\kappa}$	$\boldsymbol{\delta}$	$\boldsymbol{\epsilon}$
Baseline value	0.5	0.33	0.00971	0.00325	0.000016	0.196	0.0025	0.75
Sensitivity index	1	−0.000048	1	−0.994	−0.005	−0.9873	−0.0126	−0.0043

Discussion

There are two types of parameters in the model: controllable and non-controllable. Among them, β, α, and ϵ can be controlled. For example, β can be reduced through mask-wearing, avoiding crowded gatherings, and increasing public awareness. The parameter α can be raised by expanding vaccination campaigns, while ϵ can be improved by administering high-efficacy vaccines.

Increasing vaccination rates in Afghanistan is feasible but challenging. Limited cold-chain capacity, misinformation, and restricted access in insecure areas hinder large-scale campaigns. However, urban centers and the existing health facility network can scale distribution if supplies are stable. Community-based outreach—especially through local leaders and mobile vaccination teams—has proven effective in improving acceptance. With continued donor support and targeted delivery strategies, higher vaccination coverage remains achievable despite structural constraints.

According to sensitivity analysis section (Figure 4), the parameters β and α have the greatest impact on the system, whereas ϵ has the least influence. Therefore, interventions should primarily target reducing β and increasing α, as focusing on ϵ would yield comparatively limited results. In other words, rather than prioritizing the purchase of high-efficacy vaccines, it may be more effective to vaccinate a larger proportion of the population with lower-efficacy vaccines.

Impact of Vaccination

To evaluate the role of vaccination in mitigating the COVID-19 epidemic, we considered three simulation scenarios: (i) no vaccination (baseline), (ii) vaccination at the observed average daily coverage, and (iii) an accelerated campaign with twice the observed coverage.

In all cases, vaccine efficacy was fixed at $\epsilon = 0.75$, and vaccine doses were assumed to be distributed uniformly across all age groups. The

simulation outcomes, shown in Figure 5, demonstrate that vaccination substantially reduced peak prevalence, delayed the timing of the epidemic peak, and decreased both total cases and deaths. Among the scenarios considered, the accelerated campaign produced the most significant benefits.

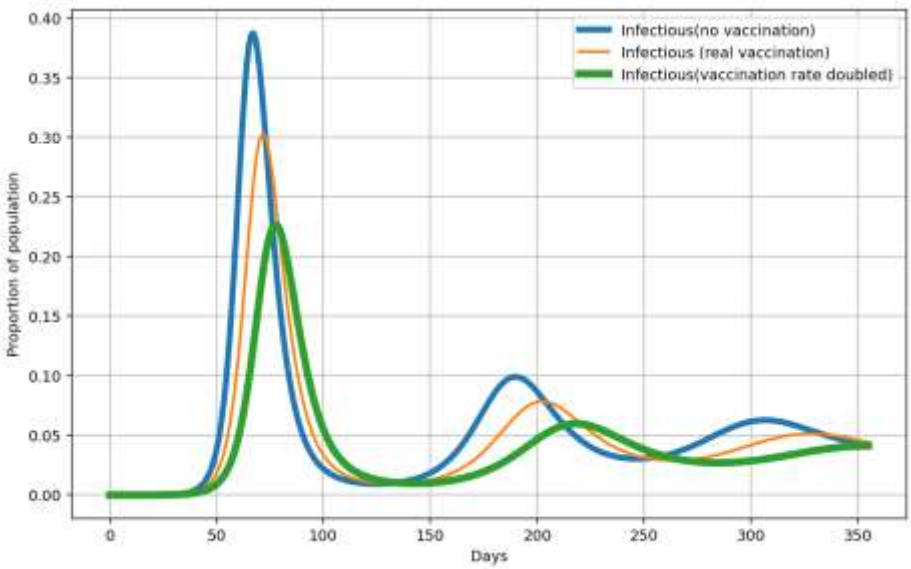

Figure 5: Comparison of different vaccination rates on COVID-19 dynamics (*The graph is obtained by numerically solving the system using the Runge-Kutta method)*

Policy Implications

Model projections indicate that doubling the current vaccination rate would reduce infections by more than 15%. Furthermore, an accelerated vaccination program would shift the epidemic peak to a later date, as illustrated in Figure 5.

Following the herd immunity framework described in (28), the minimum proportion p of susceptible individuals that must be vaccinated to interrupt transmission is given by

$$p > 1 - \frac{1}{\mathcal{R}_0} \approx 0.867.$$

This implies that approximately 86% of the population must be vaccinated to achieve long-term epidemic control.

Strengths and Limitations

A key strength of this study is the application of a mathematically rigorous framework to capture COVID-19 dynamics, with explicit incorporation of vaccination data. Additionally, the sensitivity analysis provided valuable insights into the most influential parameters, offering guidance for targeted interventions.

Nonetheless, several limitations should be acknowledged. First, the assumption of homogeneous mixing may oversimplify real-world contact patterns, given variations in population density, cultural practices, and mobility across Afghanistan. Second, parameter estimates were derived from reported data, which may be incomplete due to underreporting, limited testing, or delays in data collection. Third, the model did not account for waning immunity, reinfections, or the emergence of new variants with higher transmissibility or immune escape. Each of these factors could significantly affect projections. Furthermore, the vaccination rate was treated as constant, whereas in reality it fluctuates depending on vaccine supply and political stability.

Future Directions

Future research should extend the model by incorporating age structure, particularly relevant

for Afghanistan's young population, as well as stochastic effects to capture uncertainties in small populations or localized outbreaks. Accounting for waning immunity (assumed constant here) and booster vaccination strategies would also improve realism. Incorporating spatial heterogeneity could refine predictions by reflecting regional disparities in vaccination coverage, healthcare access, and population density. Moreover, integrating behavioral dynamics—such as vaccine hesitancy and adherence to non-pharmaceutical interventions (NPIs)—would enhance the policy relevance of the model.

Reported case data suggest a possible link between COVID-19 transmission and seasonality, with major waves often beginning in the early summer (Figure 3). This implies that transmission rates may be partially seasonal. However, the current model does not capture seasonality and cannot predict epidemic waves, which represents another limitation to be addressed in future work.

Conclusion

This study employed a compartmental model to analyze the dynamics of COVID-19 in Afghanistan, with a particular focus on the role of vaccination. Sensitivity analysis revealed that transmission rate (β) and vaccination coverage (α) are the most influential parameters, while vaccine efficacy (ϵ) has a comparatively smaller impact. These findings suggest that public health interventions should prioritize reducing transmission through non-pharmaceutical measures and expanding vaccine coverage, even if the available vaccines are of moderate efficacy.

Simulation results further demonstrated that vaccination substantially reduces peak prevalence, delays the epidemic peak, and lowers overall morbidity and mortality, with accelerated campaigns producing the greatest benefits. Policy projections indicate that approximately 86% of the population must be vaccinated to achieve herd immunity, underscoring the urgent need to strengthen vaccination programs.

Policymakers should prioritize vaccinating as many individuals as possible, even if only lower-efficacy vaccines are available. The target should be set at vaccinating approximately 86% of the population; although achieving this level may be practically challenging, approaching this threshold would still produce a substantial reduction in disease transmission and a meaningful public health impact.

Despite its strengths, including the use of real vaccination data and rigorous sensitivity analysis, the model has limitations, such as the assumption of homogeneous mixing, constant vaccination rates, and emerging variants. These factors highlight the need for more refined models that incorporate age structure, spatial heterogeneity, behavioral dynamics, and seasonality.

Overall, our results emphasize that timely expansion of vaccination coverage, supported by sustained non-pharmaceutical interventions, is the most effective strategy for long-term control of COVID-19 in Afghanistan. Future work should address the identified limitations to provide more accurate guidance for policymakers in preparing for subsequent epidemic waves.

Acknowledgments

This research did not receive any specific grant from funding agencies in the public, commercial, or not-for-profit sectors.

Conflict of interest

The authors declare no conflict of interests.

References

1. Hye MA, Biswas MHA, Uddin MF. Optimal control analysis to reduce the health complexity of co-infection with COVID-19 and kidney disease. Sci Rep. 2025 Jul 2;15(1):22845.

2. Dhand R, Li J. Coughs and sneezes: Their role in transmission of respiratory viral infections, including SARS-CoV-2. Am J Respir Crit Care Med. 2020 Sep 1;202(5):651-659.
3. Spihlman AP, Gadi N, Wu SC, Moulton VR. COVID-19 and systemic lupus erythematosus: Focus on immune response and therapeutics. Front Immunol. 2020 Oct 30;11: 589474.
4. Kong L, Duan M, Shi J, Hong J, Chang Z, Zhang Z. Compartmental structures used in modeling COVID-19: A scoping review. Infect Dis Poverty. 2022 Jun 21;11(1):72.
5. Husseini AA, Kamil AA. Estimating COVID-19 dynamics in Afghanistan. J Clin Pract Res. 2020; 42(4): 468-473.
6. World Health Organization. WHO coronavirus (COVID-19) dashboard > more resources [dashboard]. https://data.who.int/dashboards/covid19/more-resources; 2023.
7. Wang L, Khan AA, Ullah S, Haider N, AlQahtani SA, Saqib AB. A rigorous theoretical and numerical analysis of a nonlinear reaction-diffusion epidemic model pertaining dynamics of COVID-19. Sci Rep. 2024 Apr 4;14(1):7902.
8. Nemat A, Bahez A, Salih M, Raufi N, Noor NAS, Essar MY, et al. Public willingness and hesitancy to take the COVID-19 vaccine in Afghanistan. Am J Trop Med Hyg. 2021 Jul 8;105(3):713-717.
9. Blower SM, McLean AR. Prophylactic vaccines, risk behavior change, and the probability of eradicating HIV in San Francisco. Science. 1994 Sep 2;265(5177):1451-4.
10. Movaheedi Z, Sharifi AK, Safi N. Dynamics-Informed Neural Network Modeling of COVID-19 Transmission in Afghanistan Using the SEIR-V Framework. AJID. 2025 Jul. 20;3(2):177-92.
11. Awan UA, Malik MW, Khan MI, Khattak AA, Ahmed H, Hassan U, Qureshi H, Afzal MS. Predicting COVID-19 incidence in war-torn Afghanistan: A timely response is required! J Infect. 2022 Jan;84(1): e6-e8.
12. Dar JG, Ijaz M, Almanjahie IM, Farooq M, El-Morshedy M. Statistical analysis of the COVID-19 mortality rates with probability distributions: The case of Pakistan and Afghanistan. Comput Math Methods Med. 2022 Jul 25;2022: 4148801.
13. Federal Reserve Bank of St. Louis. Crude birth rate for afghanistan [Internet]. 2023 [cited 2025 Aug 15]. Available from: https://fred.stlouisfed.org/series/SPDYNCBRTINAFG
14. Macrotrends. Afghanistan Death Rate 1950–2025. Macrotrends LLC; c2025. Available from: https://www.macrotrends.net/global-metrics/countries/afg/afghanistan/death-rate
15. Polack FP, Thomas SJ, Kitchin N, Absalon J, Gurtman A, Lockhart S, et al. Safety and efficacy of the BNT162b2 mRNA covid-19 vaccine. N Engl J Med. 2020 Dec 31;383(27):2603-2615.
16. Baden LR, El Sahly HM, Essink B, Kotloff K, Frey S, Novak R, et al. Efficacy and safety of the mRNA-1273 SARS-CoV-2 vaccine. N Engl J Med. 2021 Feb 4;384(5):403-416.
17. Sadoff J, Gray G, Vandebosch AV, Cárdenas V, Shukarev G, Grinsztejn B, et al. Safety and efficacy of single-dose Ad26.COV2.s vaccine against covid-19. N Engl J Med. 2021 Jun 10;384(23):2187-2201.
18. Lauer SA, Grantz KH, Bi Q, Jones FK, Zheng Q, Meredith HR, et al. The incubation period of coronavirus disease 2019 (COVID-19) from publicly reported confirmed cases: Estimation and application. Ann Intern Med. 2020 May 5;172(9):577-582.
19. Zhang M, Xiao J, Deng A, Zhang Y, Zhuang Y, Hu T, et al. Transmission Dynamics of an Outbreak of the COVID-19 Delta Variant B.1.617.2 - Guangdong Province, China, May-June 2021. China CDC Wkly. 2021 Jul 2;3(27):584-586.
20. Backer JA, Eggink D, Andeweg SP, Veldhuijzen IK, van Maarseveen N, Vermaas K, et al. Shorter serial intervals in SARS-CoV-2 cases with Omicron BA.1 variant compared with Delta variant, the Netherlands, 13 to 26 December 2021. Euro Surveill. 2022 Feb;27(6):2200042.
21. Li Q, Guan X, Wu P, Wang X, Zhou L, Tong Y, et al. Early transmission dynamics in wuhan, china, of novel coronavirus–infected pneumonia. N Engl J Med. 2020 Mar 26;382(13):1199-1207.
22. Kucharski AJ, Russell TW, Diamond C, Liu Y, Edmunds J, Funk S, et al. Early dynamics of transmission and control of COVID-19: A mathematical modelling study. Lancet Infect Dis. 2020 May;20(5):553-558.
23. Verity R, Okell LC, Dorigatti I, Winskill P, Whittaker C, Imai N, et al. Estimates of the severity of coronavirus disease 2019: A model-based analysis. Lancet Infect Dis. 2020 Jun;20(6): 669-677.
24. He X, Lau EH, Wu P, Deng X, Wang J, Hao X, et al. Temporal dynamics in viral shedding and

transmissibility of COVID-19. Nat Med. 2020 May;26(5):672-675.
25. Li R, Pei S, Chen B, Song Y, Zhang T, Yang W, et al. Substantial undocumented infection facilitates the rapid dissemination of novel coronavirus (SARS-CoV-2). Science. 2020 May 1;368(6490):489-493.
26. Van den Driessche P. Reproduction numbers of infectious disease models. Infect Dis Model. 2017 Jun 29;2(3):288-303.
27. Diekmann O, Heesterbeek JAP, Roberts MG. The construction of next-generation matrices for compartmental epidemic models. J R Soc Interface. 2010 Jun 6;7(47):873-85.
28. Brauer F, Castillo-Chavez C, Feng Z. Mathematical models in epidemiology. New York: Springer; 2019 Feb 20.
29. Ritchie H, Mathieu E, Rodés-Guirao L, Appel C, Giattino C, Ortiz-Ospina E, et al. Coronavirus pandemic (COVID-19) [Internet]. Our World in Data. Our World in Data; 2025. Available from: https://ourworldindata.org/coronavirus
30. Linton NM, Kobayashi T, Yang Y, Hayashi K, Akhmetzhanov AR, Jung S, et al. Incubation period and other epidemiological characteristics of 2019 novel coronavirus infections with right truncation: A statistical analysis of publicly available case data. Journal of clinical medicine. 2020;9(2):538. J Clin Med. 2020 Feb 17;9(2):538.